PCCP

PROPERTIES OF TRANSITION METAL SUBSTITUTED ZINC SULFIDE HEXAMERS AND DODECAMERS

Journal:	*Physical Chemistry Chemical Physics*
Manuscript ID:	CP-ART-01-2015-000574
Article Type:	Paper
Date Submitted by the Author:	29-Jan-2015

Complete List of Authors:	Poggio, Stefano; Dartmouth College, Chemistry Wang, Brendan; Dartmouth College, Chemistry Gibson, Ursula; Norweigian Universiyt of Science and Technology, Physics BelBruno, Joseph; Darmouth College, Chemistry

PCCP Guidelines for Referees

Physical Chemistry Chemical Physics **(*PCCP*) is a high quality journal with a large international readership from many communities**

Only very important, insightful and high-quality work should be recommended for publication in *PCCP*.

To be accepted in *PCCP* - a manuscript must report:

- Very high quality, reproducible new work
- **Important new physical insights** of significant general interest
- A novel, stand-alone contribution

Routine or incremental work should not be recommended for publication. Purely synthetic work is not suitable for PCCP

If you rate the article as 'routine' yet recommend acceptance, please give specific reasons in your report.

Less than 50% of articles sent for peer review are recommended for publication in *PCCP*. The current PCCP Impact Factor is **4.20**.

PCCP is proud to be a leading journal. We thank you very much for your help in evaluating this manuscript. Your advice as a referee is greatly appreciated.

With our best wishes,

Anna Simpson (pccp@rsc.org)
Managing Editor, PCCP

Prof Daniella Goldfarb
Chair, PCCP Editorial Board

General Guidance (For further details, see the RSC's Refereeing Procedure and Policy)

Referees have the responsibility to treat the manuscript as confidential. Please be aware of our **Ethical Guidelines** which contain full information on the responsibilities of referees and authors.

When preparing your report, please:
• Comment on the originality, importance, impact and scientific reliability of the work;
• State clearly whether you would like to see the paper accepted or rejected and give detailed comments (with references) that will both help the Editor to make a decision on the paper and the authors to improve it;

Please inform the Editor if:
• There is a conflict of interest;
• There is a significant part of the work which you cannot referee with confidence;
• If the work, or a significant part of the work, has previously been published, including online publication, or if the work represents part of an unduly fragmented investigation.

When submitting your report, please:
• Provide your report rapidly and within the specified deadline, or inform the Editor immediately if you cannot do so. We welcome suggestions of alternative referees.

PROPERTIES OF TRANSITION METAL SUBSTITUTED ZINC SULFIDE HEXAMERS AND DODECAMERS

Stefano Poggio[a], Brendan Wang[a], Ursula J. Gibson[b] and Joseph J. BelBruno[a]

[a] Department of Chemistry, Dartmouth College, Hanover NH 03755 USA
[b] Department of Physics, Norwegian University of Science and Technology, 7491 Trondheim Norway

ABSTRACT

Density functional theory was used to study the structural and electronic properties of endohedrally- and substitutionally-doped Zn_6S_6 and $Zn_{12}S_{12}$ clusters with first-row transition metal atoms. Generally, the lowest energy electronic state of the cluster is that with the maximum multiplicity (Ti and Cr are exceptions). Substitutionally-doped clusters have greater binding energies for both cluster sizes, providing an indication that similar doping will be preferred in the bulk material as well. The results are relevant to thin films of doped ZnS in which cluster formation is likely.

INTRODUCTION

Chalcogenide clusters have been widely studied in our group as well as those of other researchers.[1-7] However, ZnS clusters have received less attention than, for example, those of ZnO. In particular, substitutional and endohedral doping of ZnS clusters of varying sizes is a concept that has not been fully developed or understood. Indeed, the study of these clusters could provide valuable information regarding the doping of the bulk material without the high computational cost of the direct calculation of doped semiconductor properties. If we restrict the discussion to clusters with high symmetry, then the lowest stoichiometric molecules are Zn_6S_6 and $Zn_{12}S_{12}$. The symmetry of these clusters allows for both endohedral interaction (the equivalent of interstitial doping in the bulk material) and substitutional interaction in which the transition metal (TM) atom replaces a zinc atom in the cluster structure.

Recent research involving ZnS may be grouped into three classes: (1) bulk studies, (2) applications to nanostructures and (3) clusters. Our interest is localized in the last of these groups, but since the results may be important to the bulk material, we review all three categories and compare our results to any relevant previous work. Zhang, et al.[8] reported on a first principles calculation of first row TM atom ion doping of wurtzite ZnS and observed a partially filled intermediate band for Cr, Ni and Fe, but not Mn or Co. They also reported that the stability of the wurzite and zinc blende forms of the semiconductor were approximately identical. Thin films of transition metal doped ZnS are typically polymorphic, with disordered intergrain regions [9,10], suggesting that cluster calculations may be a suitable method for elucidating the electronic and optical properties of this material. Xie[11], also based on first principles, studied the magnetic properties of Cr, Mn, Fe, Co and Ni doped ZnS and observed that doping with Cr, Fe and Ni resulted in half-metallic materials, while the remaining doped ZnS materials were semiconducting. Tablero[12] reported on the calculation of the ionization energies of TM doped ZnS and noted that doping has little effect on the lattice parameters. Akai and Ogura [13] also studied the half-metallic doped semiconductor and its magnetic properties.

Not surprisingly, semiconducting ZnS nanostructures have received considerable attention in the research community. TM-doping of ZnS quantum dots[14,15], Mn-, Cu-, Cr-, Ni- and Fe- doping of ZnS nanowires[16], TM-doping of cubic ZnS nanoparticles[17-20] and ZnS nanocrystals[21] have been reported. The magnetic and electronic properties of these nanostructures are varied and dependent on the physical identity of the transition metal atom.

The literature on TM- doped ZnS clusters has been limited to $Zn_{12}S_{12}$ and $Zn_{16}S_{16}$ material and primarily to computational studies. Matxain and co-workers have been leading the computational effort, doping the twelve-mer with both first[22,23] and second row[24] transition metal atoms. In addition, they have characterized the transition states connecting endohedral and surface doped structures. Other researchers[25] have examined the magnetic properties of singly and doubly transition metal doped ZnS.

In this report, we examine the structural and electronic properties of endohedrally- and substitutionally-doped ZnS hexamers and dodecamers with the goal of extracting information that may be applied to the general properties of the bulk semiconductor. We approach this computationally, using the PBE functional with a triple zeta plus double polarization basis set in the absence of any symmetry constraints.

THEORETICAL METHODS AND COMPUTATIONAL DETAILS

Calculations were performed using the spin-unrestricted formalism of the Amsterdam Density Functional program suite (ADF2013).[26-28] The exchange-correlation interaction utilized the generalized gradient approximation with the Perdew-Burke-Ernzerhof (PBE) functional[29] and the ADF-parameterized triplet zeta plus double polarization basis (TZ2P) set. [30]. Structures are fully optimized without any symmetry constraints and all possible spin multiplicities were treated. Only results for the multiplicity of the lowest energy clusters are reported below. The endohedral and substitutional hexamers were optimized with a gradient of 10^{-3} hartree/Å and energy change of 10^{-4} hartree, the default values in ADF. The convergence parameters for the dodecamers were 10^{-4} hartree/Å on the gradient and $5x10^{-5}$ hartree on the energy, with a geometry step of 10^{-2} Å. The singlet state of $Zn_{11}S_{12}Ti$ was optimized with a gradient

of 10^{-3} hartree/Å, while the remaining parameters were the same as for the substitutional clusters. Frequency calculations confirm that the reported geometries are indeed stationary states. Mulliken population analysis is used to determine charge and spin densities on each atom.

The stability of a cluster is conventionally described by the binding energy, which is defined as

$$E_{binding} = E_{cluster} - \Sigma E_{atoms},$$

where $E_{binding}$ is the calculated binding energy, $E_{cluster}$ is the total energy of the zinc sulfide cluster and the summation is over the atomic energy of all of the cluster atoms. Negative binding energies reflect a stable conformation.

RESULTS and DISCUSSION

For computational comparison, the electronic properties of the parent clusters, Zn_6S_6 and $Zn_{12}S_{12}$, were determined. The binding energies were 31.2 eV and 66.5 eV, while the HOMO-LUMO gaps were 2.59 eV and 3.36 eV, respectively for the hexamer and dodecamer. The differences between the cluster gaps and the band gap of bulk ZnS are readily ascribed to the effect of size-the HOMO-LUMO gap trends towards the band gap value as the cluster size grows larger.

Hexamers. The ground state geometry was considered for endohedral, TM@Zn_6S_6, and substitutional, Zn_5S_6TM, doping. All possible spin states, based on the total electron distribution *within the cluster*, were examined and only the lowest energy state for the molecule is reported here. For the hexamers, the lowest energy endohedral cluster had the maximum transition metal atom spin state consistent with the atom present in a pseudo-symmetric field exerted by the ZnS cluster and for all of the hexamers, the endohedral TM atom was located at the center of the cluster.The symmetric field assumption is consistent with the optimized geometry where the endohedral metal atom is located at the center of, for most of the hexamers, a minimally distorted molecular cluster. The optimized endohedral geometries are similar to the geometry of the parent cluster, but the presence of the TM atom at the center of the cavity causes small

distortions. The cavity space in the parent hexamer cluster is essentially the Zn-S inter-ring distance of 2.46Å and the TM atom, depending upon its size and spin density has the potential to modify that spacing. Interestingly, the structure of the two rings comprising the ZnS hexamer shell is significantly distorted when the transition metal atom is Ni or Cr. This indicates that these two metals have a more significant interaction with the atoms in the ZnS shell. Coincidentally, these are the two transition metals in which the 4s electrons are unpaired, with the second nominally 4s electron located in a 3d orbital: the configurations are $4s3d^5$ and $4s3d^9$, respectively for Cr and Ni. The geometries for these clusters exhibit rings that are elongated compared with the remaining clusters in the series; one of the Zn-S-Zn bond angles is increased, a second is reduced and the TM-S and TM-Zn distances are shorter than in the other clusters, except for a single TM-S distance that is greater than 3Å, indicating no transition metal-sulfur interaction with this particular atom. The effect is evident in Figure 1,where the nickel doped and iron doped structures are shown as examples of this ring elongation and typical behavior, respectively, with the parent cluster. All of the

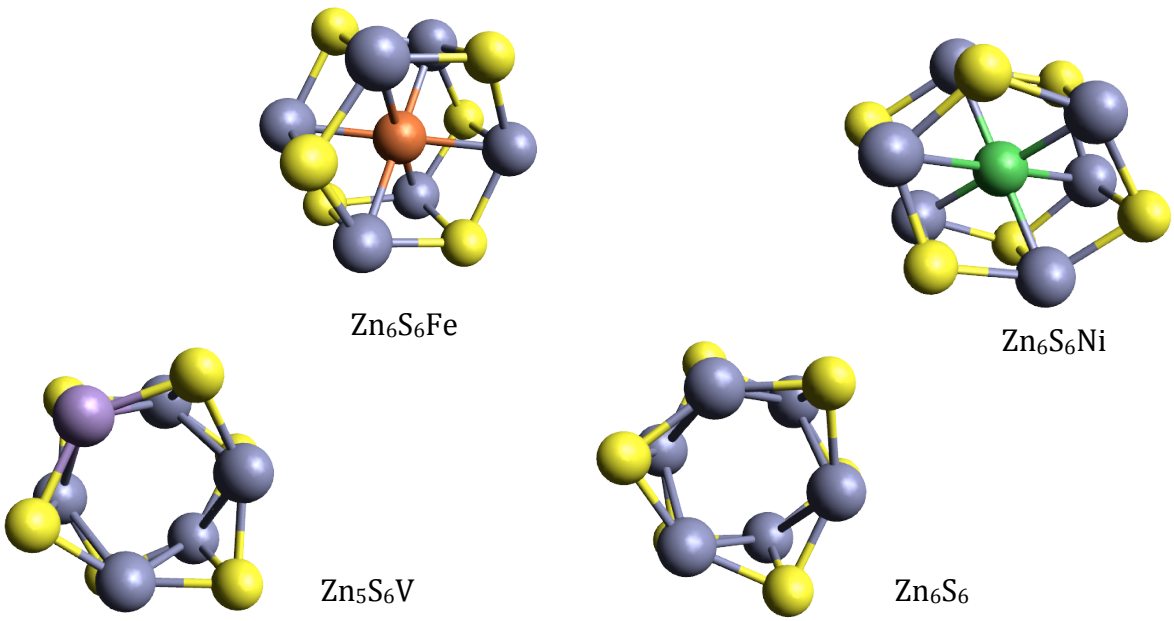

Figure 1. Representative structures for the endohedrally and substitutionally doped zinc sulfide hexamer clusters, along with the parent cluster.

bondlengths are presented in Table 1. The TM-S and TM-Zn distances are, as expected,

dependent upon the specific TM atom. However, with the exception of Ti, the effect of the endohedral TM atom is to increase the Zn-S intra-ring distance to approximately ~2.4Å from ~2.3Å, while the inter-ring Zn-S bondlength remains effectively unchanged.

The substitution of a divalent transition metal for a Zn^{2+} in the hexamer also results in a cluster with the maximum spin multiplicity, except for the Ti- and Cr- complexes. The lowest energy Ti-substituted cluster is a singlet, while the lowest energy Cr-cluster is a quintet. For the substitutionally doped clusters, the inter-ring distance is essentially identical to that of the parent cluster, ~2.48Å. The TM atom does have an effect on the ring in which it is situated. The TM-S bondlength is approximately constant below Z = 25, and then again constant, at a slightly (~4%) smaller value, for larger Z. The S-TM-S bond angle is approximately 142° across all of the transition metals, but significantly

Table 1. Bondlengths/bond angles for the doped zinc sulfide hexamer clusters.

$TM@Zn_6S_6$	**None**	**Ti**	**V**	**Cr**	**Mn**	**Fe**	**Co**	**Ni**
r, Zn-S, Å	2.29	2.65	2.38	2.40	2.40	2.36	2.35	2.34
	2.46	2.64	2.44	2.48	2.44	2.42	2.42	2.41
r, TM-S, Å	-	2.42	2.64	2.50/3.08	2.71	2.79	2.75	2.58/3.13
r, TM-Zn, Å	-	2.72	2.70	2.63/2.69	2.66	2.50	2.49	2.56/2.36
<S-Zn-S, °	142	114	114	120/111	118	126	127	114/135
<S-TM-S, °	93	126	125	109/130	121	112	111	118/96

Zn_5S_6TM	**None**	**Ti**	**V**	**Cr**	**Mn**	**Fe**	**Co**	**Ni**
r, Zn-S, Å	2.29	2.28	2.29	2.29	2.28	2.29	2.29	2.29
	2.46	2.49	2.48	2.46	2.47	2.46	2.47	2.47
r, TM-S, Å	-	2.35/2.41	2.31/2.35	2.36/2.39	2.35	2.26/2.40	2.23/2/39	2.24/2.33
r, TM-Zn, Å		2.84	2.67	2.85	2.87	2.73	2.70	2.81
<S-Zn-S, °	142	144	146	143	142	142	141	141
<S-TM-S, °	93	130	134	148	134	139	136	129

greater than the 93° angle in the parent cluster. A representative structure, Zn_5S_6V, is shown Figure 1 and additional structural information is provided in Table 1.

Table 2 contains electronic data for both the endohedral and substitutional clusters. The binding energy and the HOMO-LUMO gap were calculated for all multiplicities of the doped clusters and the results are shown in Table 2 for the lowest energy clusters. The endohedral clusters all have the maximum spin multiplicity, a trend also followed by the substitutionally doped clusters with the exception of Ti and Cr, which in the hexamer case, have the lower and unexpected singlet and quintet multiplicities, respectively. The binding energies for the substitutionally doped clusters are greater than those for the endohedrally doped molecules, indicating the substitutional doping is preferred in

Table 2. Binding energies, in eV, HOMO-LUMO gaps in eV, Mulliken spin densities, charges and binding energy differences, in eV, for the doped zinc sulfide hexamer clusters. Spin multiplicities, 2S+1, of the lowest energy clusters are shown in parentheses; endohedral Ti and Cr exhibit different spin states shown in the body of the table.

Zn_6S_6, Dopant	**None(1)**	**Ti(3)**	**V(4)**	**Cr(7)**	**Mn(6)**	**Fe(5)**	**Co(4)**	**Ni(3)**
(endohedral)								
$E_{binding}$	-31.2	-34.3	-34.4	-30.4	-31.2	-32.7	-33.7	-32.4
HOMO-LUMO	2.59	0.68	0.75	0.49	1.01	0.63	1.06	0.98
TM spin density	-	1.65	2.88	3.75	4.39	2.72	1.60	0.51
TM charge	-	0.17	0.23	0.07	0.28	0.16	0.16	0.15
(substituted)		Ti(1)		Cr(5)				
$E_{binding}$	-31.2	-35.8	-35.7	-33.0	-33.5	-34.3	-34.6	-33.3
HOMO-LUMO	2.59	0.43	0.78	0.86	2.00	0.10	0.45	0.76
TM spin density	-	0.00	2.94	4.02	4.65	3.40	2.26	1.25
TM charge	-	0.26	0.27	0.28	0.33	0.17	0.11	0.14
$E_{sub} - E_{endo}$	-	-1.5	-1.3	-2.6	-2.3	-1.6	-0.9	-0.9

clusters and, speculatively, over interstitial doping in the bulk material. Both sets of TM-containing clusters have greater binding energy than the parent cluster reflecting the stronger TM-S over the Zn-S interaction. The HOMO-LUMO gaps for the TM-containing

clusters are less than that of the Zn_6S_6 cluster and there is no coherent pattern when comparing the endohedral and substitutional TM-clusters. A smaller HOMO-LUMO gap, relative to the bulk band gap, is usually attributed to the quantum size effect, with the HOMO-LUMO gap trending towards the bulk band gap as the cluster increases in diameter for larger clusters. A larger gap is reflective of greater chemical stability, indicating that the $Mn@Zn_6S_6$ and Zn_5S_6Mn clusters are the most chemically stable of the endohedral and substituted hexamer clusters, respectively, explored in this study.

All of the TM atoms exhibit a small Mulliken charge. Also, the data in Table 2 show that, like endohedral carbon fullerene complexes in which the endohedral atom retains its free-space spin density, the TM atoms in the endohedral hexamers almost all have spin densities approximately equal to the number of unpaired electrons in the free atom. This observation, that the spin density is localized on the TM atom, indicates that the metal atom is not chemically interacting with the zinc sulfide cluster and is effectively trapped, even in such a small molecular cage. The two endohedral TM cluster exceptions are those for Cr and Ni. On a percentage basis, the transfer of spin density away from the metal atom is most significant for these two TMs, presumably, due to electronic interactions with the cage. This interaction was presaged by the structural data in Table 1, in which both of these hexamer clusters caused significant geometric distortions relative to the structure of parent cluster. The charge on the transition metal is relatively constant for Ti through Mn and again, although slightly lower, for Fe through Ni. There are no computational or experimental data for the hexamer clusters, precluding any comparison.

Dodecamers. The ground state geometry was also considered for the larger endohedral $TM@Zn_{12}S_{12}$ and substitutional $Zn_{11}S_{12}TM$ clusters. Table 3 presents the distinguishing geometric features of the clusters; the location of the transition metal atom for the endohedral clusters and the bondlengths/bond angles involving the TM atom for the substituted 12-mers. Table 4 shows the binding energies of both sets of clusters along with their HOMO-LUMO gap and the Mulliken population analysis. We found, consistent with the hexamer results, that the lowest energy endohedral geometry included the TM atom with the highest possible spin multiplicity. The transition metal atom in the

endohedral clusters did not universally remain at the center of the cluster after structural optimization. In particular, the Ti, V, Ni and Fe atoms in the TM@$Zn_{12}S_{12}$ clusters were

Table 3. Geometric parameters for the lowest energy12-mers: location of the TM atom from the center of the cage for TM@$Zn_{12}S_{12}$ and TM-S bondlengths/S-TM-S bond angles for the substituted cluster.

TM@$Zn_{12}S_{12}$	**None**	**Ti**	**V**	**Cr**	**Mn**	**Fe**	**Co**	**Ni**
(endohedral)								
Location, Å	-	1.07	1.10	0.04	0.03	1.08	0.04	1.40
(substituted)								
$Zn_{11}S_{12}$TM	*Zn-S*							
S-TM, Å	2.34	2.25	2.38	2.38	2.39	2.30	2.29	2.26
	2.34	2.25	2.38	2.33	2.39	2.30	2.29	2.26
	2.25	2.33	2.35	2.34	2.32	2.25	2.20	2.20
<S-TM-S, °	98	108	98	94	97	101	100	102
	130	125	123	119	128	129	130	124
	130	125	123	147	128	129	129	124

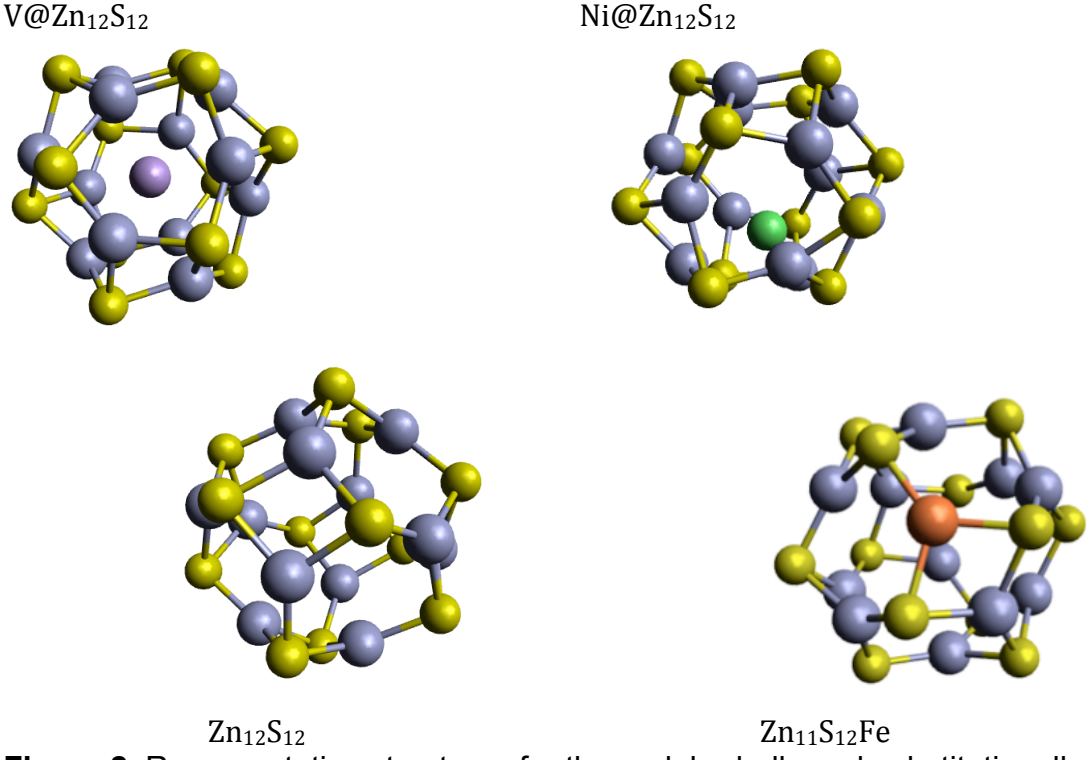

Figure 2. Representative structures for the endohedrally and substitutionally doped zinc sulfide dodecamers, along with the parent cluster.

optimized to a geometry with the TM atom located approximately 1Å away from the center of the cluster. In the remaining clusters, the Cr, Mn and Co atoms were essentially located at the origin. The geometry of the ZnS portion of the cluster in these endohedral complexes was unperturbed relative to the parent cluster. The structural results are mostly consistent with the single previous study that examined the set of endohedral cluster geometries.[22] The shift of the endohedral atom was slightly less in that study and the Co atom was found to shift, whereas in our study, the Co atom remains at the origin and the Fe atom shifts off center. The difference may possibly be attributed to the difference in theoretical model, but Matxain's group used transition metal atoms with the maximum possible number of unpaired electrons, while we maximized the spin on the cluster as a whole. The parent cluster, $Fe@Zn_{12}S_{12}$ and $Co@Zn_{12}S_{12}$ cluster geometries are shown Figure 2 as representative samples. The transition metal atom substituted dodecamer clusters maintain the approximate symmetry of the parent cluster, however, the TM-S bondlengths and bond angles do undergo slight changes, in agreement with Chen's results.[25] We note that there are two distinct bondlengths in the parent molecule; 2.34Å and 2.25Å. Table 4 shows that the doubly equivalent TM-S bondlength increases across the transition metal period starting at Ti to a maximum at Mn followed by a decrease to nickel, while the remaining bondlength begins with an significant increase over the parent molecule for Ti and decreases across the entire period. Bond angles, with the exception of those in the Cr-substituted structure, which has three very different bond angles compared with the other clusters with only two unique angles, are not significantly different from those of the parent cluster.

The electronic data in Table 4 show some similarities and some differences with respect to the analogous hexamer data. Just as with the hexamer clusters, the singlet state of $Zn_{11}S_{12}Ti$ was found to be lower (by 0.17 eV) in energy than the corresponding triplet, which was the ground spin state for the endohedral $Ti@Zn_{12}S_{12}$ cluster. Likewise, the quintet state of $Zn_{11}S_{12}Cr$ was lower (by 2.30 eV) in energy than the septet. The binding energies of the endohedral clusters are all less than those of the substitutionally doped clusters; in agreement with the smaller clusters. In addition, the bond energies of

the substituted clusters are all greater than that of the parent molecule, but the HOMO-LUMO gaps for the TM-containing clusters are less than that of the parent cluster. Based on the size of the HOMO-LUMO gap, the $Cr@Zn_{12}S_{12}$ and $Zn_{11}S_{12}Mn$ clusters are the most chemically stable among their respective class of cluster. The endohedral clusters have very small charges on the TM atoms, which grow larger in moving to the substituted clusters. Spin density remains, primarily, on the transition metal atom, however, the heavier TM atom containing clusters, Fe-, Co- and Ni-substituted dodecamers, exhibit more significant loss of spin density compared to the other clusters.

Table 4. Binding energies, in eV, HOMO-LUMO gaps in eV, Mulliken spin densities and charges for the doped zinc sulfide dodecamer clusters. Spin multiplicities, 2S+1, are shown in parentheses.

$Zn_{12}S_{12}$, Dopant	**None(1)**	**Ti(3)**	**V(4)**	**Cr(7)**	**Mn(6)**	**Fe(5)**	**Co(4)**	**Ni(3)**
(*endohedral*)								
$E_{binding}$	-66.50	-68.87	-69.23	-67.69	-67.49	-68.67	-69.25	-68.47
HOMO-LUMO	3.360	0.982	0.936	2.167	0.475	1.835	0.602	1.280
TM spin density		1.835	3.006	5.402	4.789	3.744	2.608	1.488
TM charge		-0.185	-0.205	0.139	-0.001	-0.247	-0.010	-0.468
(*substituted*)		*Ti(1)*		*Cr(5)*				
$E_{binding}$	-66.50	-70.90	-70.66	-68.08	-68.65	-69.51	-69.77	-68.38
HOMO-LUMO	3.360	1.343	0.752	1.057	2.567	1.008	0.773	0.752
TM spin density		0	3.043	4.043	4.688	3.438	2.343	1.277
TM charge		0.242	0.348	0.271	0.351	0.170	0.120	0.140
$E_{sub} - E_{endo}$	-	-2.03	-1.43	-0.39	-1.16	-0.84	-0.52	0.09

General comments. We noted in the discussion of the hexamers, that one might infer that the greater stability of the TM-substituted clusters (over the endohedral clusters) indicated that substitutional rather than interstitial doping would be preferred in the bulk material. Continuing with the connection of the clusters to bulk properties, Figure 3 presents the energy levels of the highest occupied and lowest vacant orbitals with reference to the primary atomic contribution to the orbital. In the figure, the highest occupied MOs and lowest unoccupied orbitals from the ZnS cluster atoms are shown in yellow and green, respectively. Note that the energy difference between these two levels does undergo any significant variation across the figure. The absolute HOMOs,

primarily comprised of TM *d*-orbitals, are shown in red and the unoccupied *d*-orbitals are shown in blue. If one treat the levels as would be done in the bulk, that is, consider the ZnS HOMO as the valence band, the ZnS LUMO as the conduction band and the TM-orbitals as *n*-type dopant levels in the band gap, the difference between the highest energy, occupied TM-orbital and the ZnS LUMO is the doped 'band gap'. These energy differences should be related to the photoexcitation of carriers to the conduction band of ZnS films containing defect structures similar to the clusters presented here. We

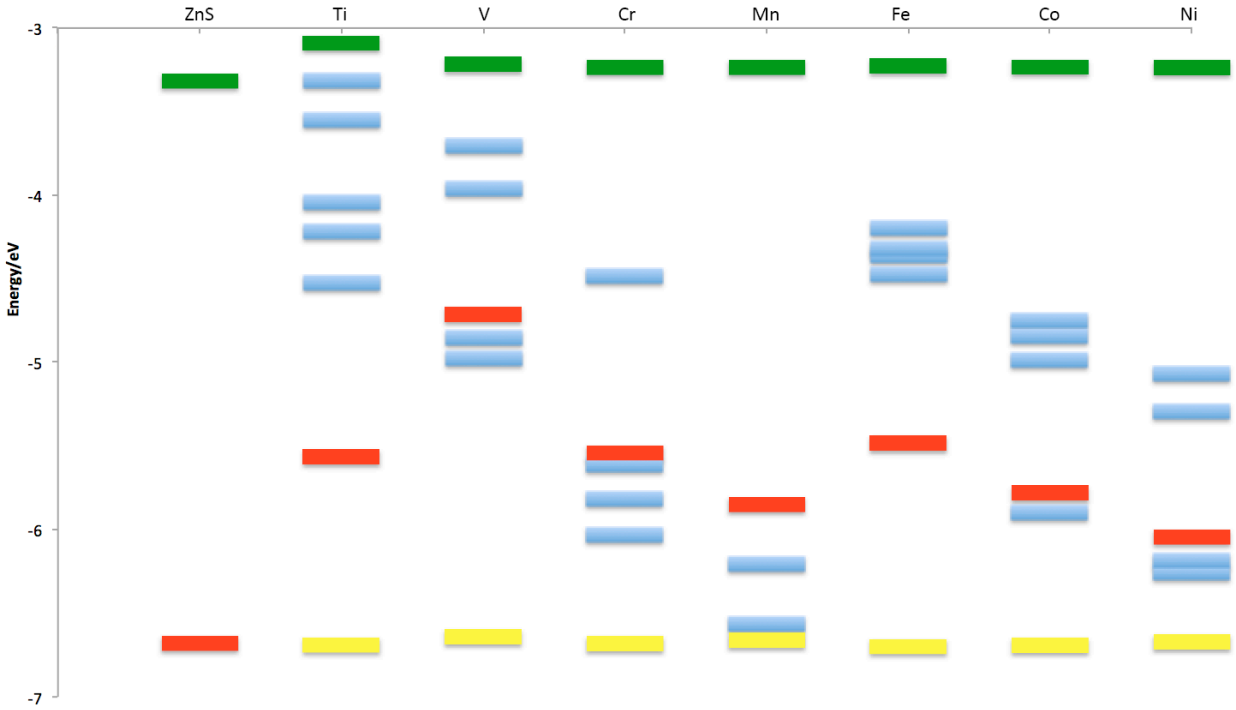

Figure 3. Calculated MO energy levels for the TM-substituted dodecamer clusters.

have chosen to use the dodecamer data, since the larger clusters are trending towards the bulk properties, however, the hexamer data present similar results. The energy differences calculated for the dodecamer are shown in Figure 4. These results suggest that vanadium and iron present the opportunity for lower band gaps, while the other transition metals potentially offer approximately a 25% reduction in the bulk band gap. The choice of dopant, then, can be based on the compatibility of the total system.

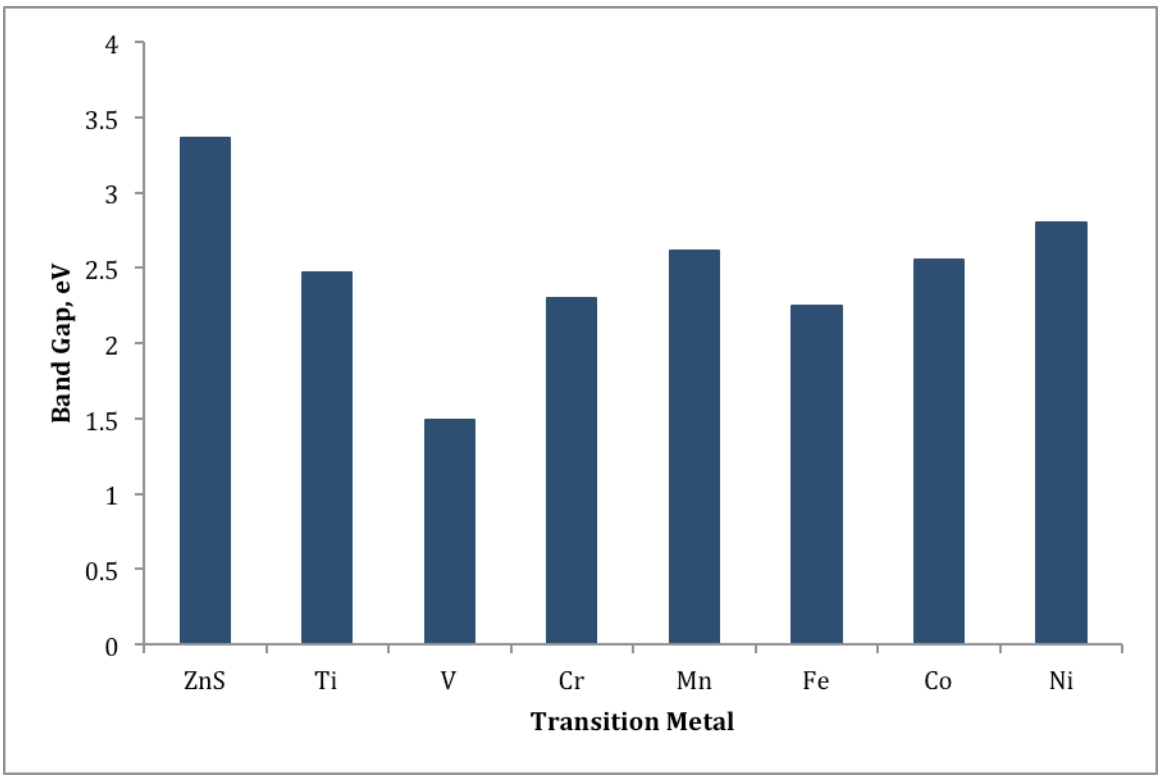

Figure 4. Calculated 'band gaps' for the TM-substituted dodecamer clusters.

Acknowledgements
The authors acknowledge the support of both NOTUR through project number NN9291K and NFR via grant 219686/O70.

References

1. J.M. Matxain, J.E. Fowler and J.M Ugalde, "Small clusters of II-VI materials: Zn_iO_i, i=1-9" *Phys. Rev. A* **61** (2000) 053201/1-053201/10.

2. E. Spano, S. Hamad and C.R.A. Catlow, "Computational evidence of bubble ZnS clusters" *J. Phys. Chem.* **B107** (2003) 10337-10340.

3. E. Spano, S. Hamad and C.R.A. Catlow, "ZnS bubble clusters with onion-like structures" *Chem. Comm.* **7** (2004) 864-865.

4. J. Muilu and T.A. Pakkanen, "Ab initio study of small zinc sulfide crystallites", *Surf. Sci.* **364** (1996) 439-452.

5. S.M. Woodley, A.A. Sokol and C.R.A. Catlow, “Structure prediction of inorganic nanoparticles with predefined architecture using a genetic algorithm” *Zeit. Anorgan. Allgem. Chem.* **630** (2004) 2343-2353.

6. T.P. Martin, *Phys. Rep.* “Shells of atoms”, ***273*** (1996) 199-241.

7. A. Burnin and J.J. BelBruno, “$Zn_nS_m^+$ cluster production by laser ablation” *Chem. Phys. Lett.* ***362*** (2002) 341-348.

8. J.H. Zhang, J.W. Ding, J.X. Cao and Y.L. Zhang, Infrared, visible and ultraviolet absorptions of transition metal doped ZnS crystals with spin-polarized bands”, *J. Solid State Chem.* **184** (2011) 477-480.

9. D. Yoo, M.S. Choi, S.C. Heo, C. Chung, D. Kim, C. Choi, “Structural, optical and chemical analysis of zinc sulfide thin film deposited by RF-mganetron sputtering and post deposition annealing”, *Met. Mater. Int.* **19** (2013) 1309–1316.

10. J.E. Yu, K.S. Jones, J. Fang, P.H. Holloway, B. Pathangey, E. Bretschneider, et al., “Characterization of ZnS Layers Grown by MOCVD for Thin Film Electroluminescence (TFEL) Devices”, in: *Symp. G – Wide Band-Gap Semicond.*, 1992. doi:10.1557/PROC-242-215.

11. J. Xie, “First-principles study on the magnetism in ZnS-based diluted magnetic semiconductors”, *J. Mag. Mag. Mater.* **322** (2010) L37-L41.

12. C. Tablero, “Static and dynamic ionization levels of transition metal-doped zinc chalcogenides”, *Theor. Chem. Acc.* **125** (2010) 23-34.

13. H. Akai and M. Ogura, “Half-metallic diluted antiferromagnetic semiconductors”, *Phys. Rev. Lett.* **97** (2006) 026401/1-026401/4.

14. E. Sotelo-Gonzalez, L. Roces, S. Garcia-Granda, M.T. Fernandez-Arguelles, J.M. Costa-Fernandez and A. Sanz-Medel, “Influence of Mn^{2+} concentration on Mn^{2+}-doped ZnS quantum dot synthesis: evaluation of the structural and photoluminescent properties”, *Nanoscale* **5** (2013) 9156-9161.

15. S.M.T. Otaqsara, “Tunable visible emission of TM-doped ZnS quantum dots”, *Eur. Phys. J.: Appl. Phys.* **59** (2012) 10404/1-10404/6.

16. H. Chen, D. Shi and J. Qi, “Comparative studies on the magnetic properties of ZnS nanowires doped with transition metal atoms”, *J. Appl. Phys.* **109** (2011) 084338/1-085338/9.

17. V. Ramasamy, K. Praba and G. Murugadoss, “Synthesis and study of optical properties of transition metal doped ZnS nanoparticles”, *Spectrochem. Acta* **A96** (2012) 963-971.

18. D. Sridevi and K.V. Rajendran, “Enhanced photoluminescence of ZnS nanoparticles doped with transition and rare earth metallic ions”, *Chalcogen. Lett.* **7** (2010) 397-401.

19. H. Hu and W. Zhang, “Synthesis and properties of transition metals doped ZnS nanoparticles”, *Opt. Mater.* **28** (2006) 536-550.

20. D.D. Sarma, R. Viswanatha, S. Sapra, A. Prakash and M. Garcia-Hernandez, “Magnetic properties of doped II-VI semiconductor nanocrystals”, *J. Nanosci. Nanotech.* **5** (2005) 1503-1508.

21. N.S. Karan, D.D. Sarma, R.M. Kadam and N. Pradhan, “Doping transition metal (Mn or Cu) ions in semiconductor nanocrystals”, *J. Phys. Chem, Lett.* **1** (2010) 2863-2866.

22. J.M. Matxain, E. Formoso, J.M. Mercero, M. Piris, X. Lopez and J.S. Ugalde, “Magnetic endohedral transition-metal-doped semiconducting-nanoclusters”, **14** (2008) 8547-8554.

23. E. Jimenez-Izal, J.M. Matxain, M. Piris and J.M. Ulgade, “Thermal stability of endohedral first-row transition-metal TM@Zn_iS_i structures, i=12, 16”, **115** (2011) 7829-7835.

24. E. Jimenez-Izal, J.M. Matxain, M. Piris and J.M. Ulgade, “Second-row transition-metal doping of (Zn_iS_i), i=12,16 nanoclusters: structural and magnetic properties”, *Computation* **1** (2013) 31-45.

25. H. Chen, D. Shi, J. Qi and B. Wang, “First-principles study on the magnetic properties of transition-metal atoms doped $(ZnS)_{12}$ cluster”, *J. Mag. Mag. Mater.* **323** (2011) 781-788.

26. G. te Velde, F.M. Bickelhaupt, S.J.A. van Gisbergen, C. Fonseca Guerra, E.J. Baerends, J.G. Snijders and T. Ziegler, “Chemistry with ADF”, *J. Comp. Chem*. **22** (2001) 931-967.

27. C. Fonseca Guerra, J.G. Snijders, G. te Velde and E.J. Baerends, Towards an order-N DFT method, *Theor. Chem, Acc.* **99** (1998) 391-403.

28. ADF2013, SCM, Theoretical Chemistry, Vrije Universiteit, Amsterdam, The Netherlands, http://www.scm.com

29. J. P. Perdew, K. Burke, and M. Ernzerhof, “Generalized gradient approximation made simple,” *Phys. Rev. Lett.*, **77** (1996) 3865-68.

30. E. van Lenthe and E.J. Baerends, “Optimized Slater-type basis sets for the elements 1-118”, *J. Comp. Chem*. **24** (2003) 1142-1156.